GRAIN BOUNDARY MELTING IN Al-Cu-Mg ALLOY WELDS

Philip B. PRANGNELL and Andrew F. NORMAN

Manchester Materials Science Centre, University of Manchester / UMIST
Grosvenor Street, Manchester, M1 7HS, U.K.

ABSTRACT Two different fusion welding processes of TIG and YAG Laser were used to investigate the heat affected zones and the extent of grain boundary melting in the commercial aluminium alloy 2024. Grain boundary melting was observed in all the weld samples and was associated with the formation of a precipitate free zone and coarse spherical particles of the equilibrium S phase. The focused power source, and associated high cooling rates of laser welding, produced a narrow region of grain boundary melting (100-200 μm) whereas a wide region of grain boundary melting (~ 500 μm) was observed in the TIG welds. Thermal models were used to predict the correct trend of grain boundary melting with welding technique and processing parameter. However some difficulties were encountered in accurately predicting the width of the region for the different processing conditions.

Keywords: *Grain boundary melting, Al-Cu-Mg, TIG, Laser Beam, HAZ, TEM.*

1. INTRODUCTION

In recent years, the fusion welding of commercial aluminium alloys (including the AA2000 and AA7000 series) has received renewed attention [1,2]. The majority of published research has focused on relating the parameters of TIG welding to the weld metal microstructures that form in the fusion zone [1-4]. Only recently has the laser welding of commercial aluminium alloys been considered as a viable method for producing high quality structural joints [5]. Previously, there has only been a limited number of studies which have attempted to understand the development of heat affected zones (HAZs) in high strength commercial aluminium alloys [1,6]. This is primarily due to the fact that in the HAZ, the peak temperature decreases with increasing distance from the fusion zone which produces many complex metallurgical reactions in these alloys [6].

In the fusion welding of aluminium alloys, there is the possibility of forming a narrow region adjacent to the fusion zone in which the phenomenon of partial melting occurs at the grain boundaries (also known as grain boundary melting). In this region, the peak temperature lies somewhere between the solidus and liquidus of the alloy. The commercial aluminium alloy AA2024 is particularly susceptible to forming a region of grain boundary melting as it has a wide freezing range (reported to be 140°C [7]) and the potential to form a low melting point eutectic phase at around 500°C [8]. Clearly the presence of such a zone could have a detrimental effect on the mechanical performance of the weld.

In this paper, two quite distinct fusion welding processes were used to produce autogenous butt welds of the alloy AA2024. The technique of TIG welding produces wide welds due to the spread of the arc and associated low power densities. In sharp contrast, the more novel technique of laser welding utilises a highly focused beam to penetrate the sample surface. The heat inputs for laser welding are much higher compared to TIG welding, and so produce narrow welds with severe thermal cycles of heating and cooling. The main objective of this paper is to study the formation of grain boundary melting, and to see to what extent the different welding processes influence the severity of the this region, and whether it can be predicted using thermal models. For both welding techniques, the HAZs were characterised using a combination of metallographic processes; optical metallography, scanning electron microscopy (SEM), and transmission electron microscopy (TEM). The width of the region of grain boundary melting was measured for the different welding

conditions and the results are compared to thermal models which predict the heating and cooling cycle in the HAZ, for each welding process.

2. EXPERIMENTAL

The commercial aluminium alloy AA2024 (Al-4.4wt.%Cu-1.5wt.%Mg-0.8wt.%Mn + impurities of Fe and Si) was laser beam and TIG welded using the conditions given in Table 1. The sheet thickness was 1.6 mm and a simple butt geometry was used for each experiment. For the TIG welds, the speeds considered were in the range 7 to 25 mm s^{-1} and, as the welding speed was increased, the welding current was also increased to just maintain full penetration. For the laser welding, a YAG laser was used to produce welds in the range 33 to 100 mm s^{-1}, which required laser power of between 2 and 4 kW to achieve full penetration. After welding, each sample was sectioned, mounted and examined using conventional optical metallography. Samples for TEM examination were prepared from the welds by punching 3 mm discs from different positions in the HAZ. The discs were ground to a thickness of ~ 100 μm and jet-polished using a solution of 30 vol.% Nitric Acid in Methanol at –30°C and 12 V. The foils were examined in a Phillips CM20 analytical TEM operated at 200 kV.

Table 1: *Welding conditions for the samples under investigation.*

Process	Speed (mm s^{-1})	Current (A)	Power (W)	Process	Speed (mm s^{-1})	Power (W)
TIG	7	100	630[a]	Laser	33	2000
TIG	13	130	819[a]	Laser	66	3000
TIG	19	160	1008[a]	Laser	100	4000
TIG	25	190	1197[a]			

[a]calculated from $Q = \eta IV$, where Q is the total power input, I is the welding current, V is the welding voltage, and η is taken to be 0.70 [2].

3. Results and Discussion

3.1 General Description of the HAZ

The heat affected zones were characterised in an earlier paper [6] using a combination of hardness testing, optical and electron microscopy studies. Hardness profiles were produced for both welding processes as a function of distance from the weld centreline (Fig. 1). The widths of the HAZ of the TIG welds were wide (~ 20 mm from the weld centreline), compared to the laser welds which were much narrower in width. However, whilst there was some variability in hardness measurements between samples, some features of the hardness profiles were common to both welding techniques.

(i) The lowest hardness was observed in the weld (zone I), and was due to rejection of solute during solidification resulting in a coarse heavily segregated microstructure.

(ii) As the hardness profile travelled into the HAZ (zone II), the peak temperature falls below the solidus of the alloy but stays above the solvus temperature of the main strengthening phase, S′. Providing the cooling rate is sufficient to retain the solute in solid solution, natural ageing can occur which will restore the base metal properties and give rise to the first peak seen in Fig. 1.

(iii) At further distances into the HAZ (zone III), the peak temperature drops below the solvus temperature of the S′ phase, and providing the temperature remains above ~ 200°C, any

precipitates present in the matrix will coarsen, produce an overaged microstructure and a drop in hardness.

(iv) As the hardness recovers to the base metal value, there is also some evidence to suggest that a second peak is produced (zone IV). This might occur when the peak temperature lies in the range 150 to 200°C, which is the temperature range required to allow precipitation of the main strengthening phase in 2024. However the length of time at which this temperature range occurs will be quite short and depend on the welding process.

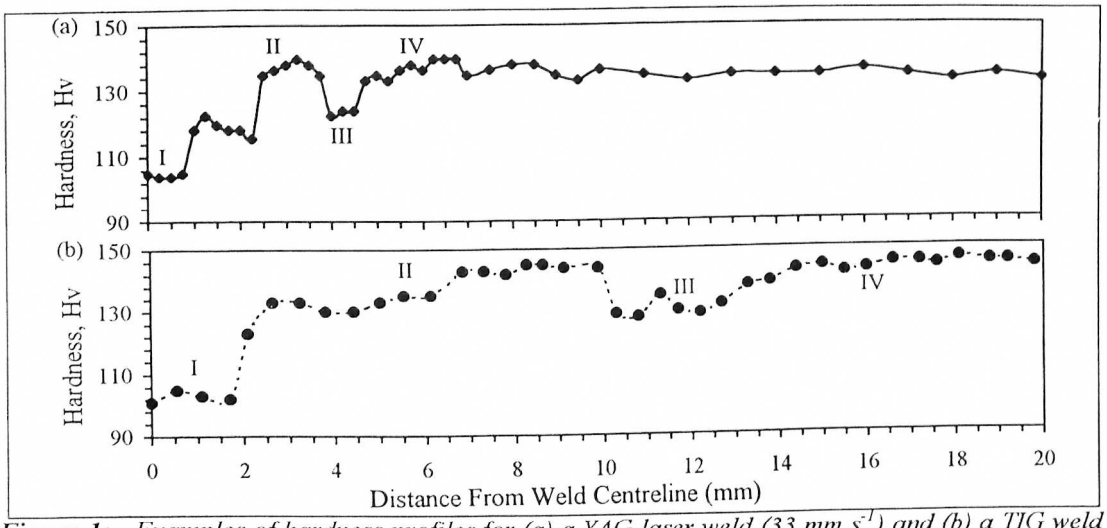

Figure 1: *Examples of hardness profiles for (a) a YAG laser weld (33 mm s^{-1}) and (b) a TIG weld (7 mm s^{-1}).*

3.2 Region of Partial Melting

In an earlier paper [6], we reported some preliminary microstructural observations on the HAZ for TIG welded 2024. SEM investigations revealed that in a narrow region adjacent to the fusion zone, a continuous eutectic film was observed at many of the grain boundaries. For the TIG welds, the film width varied from ~ 350 μm at the lowest welding speed to 500 μm for the highest speed considered. Although a similar continuous film was observed for the laser weld samples, the width of the continuous film was much narrower and varied between 100 and 200 μm depending on the welding conditions. To gain a better understanding of this microstructural zone, the weld samples were studied using TEM. An example of the zone of partial melting is shown in Fig. 2 for one of the laser welds. This montage of micrographs shows the fusion zone with the formation of the eutectic in the interdendritic regions (right hand side of the figure). and the film of eutectic at the grain boundary together with coarse spherical precipitates (left hand side).

For the continuous film to form, the temperature must exceed the melting point of the eutectic phases at the grain boundaries, which then melt locally and spread inwards to an extent depending on the peak temperature. On cooling, the liquid re-solidifies and a precipitate free zone (PFZ) is established adjacent to many of the grain boundaries due to solute rejection on freezing. This is illustrated in Fig. 3 which shows the formation of the PFZ and a solute profile across the PFZ. Also shown in Fig. 3 are the two types of precipitate which are present in both the TIG and laser welds. The coarse spherical precipitates belong to the Al_2CuMg (S) phase and form during the heating cycle. The second type of precipitates are significantly smaller, rectangular in morphology, and are the Mn-rich dispersoid phase which is present in base alloy. Although not shown here, as the distance from the fusion boundary is increased, the size and volume fraction of the S phase

decreases. This occurs over a narrow width for the laser welds, whereas for the TIG welds, coa particles of the S phase were found at distances of up to 500 μm from the fusion boundary.

Figure 2: *TEM micrographs showing the fusion zone, fusion boundary and evidence for gra boundary melting in a Laser weld (welding speed = 33 mm s^{-1}).*

The width of the region of grain boundary melting can be estimated using thermal models predict the thermal cycles which are present in the HAZ, providing the melting point of the eutec phases are accurately known. For TIG welding, it is possible to use the Rosenthal thin plate solution [9] which describes the local thermal cycle in the HAZ as a function of distance from the heat source and from the weld centreline. Although there are many assumptions that need to be made (for example, the heat source is taken to be a discrete line, the plate is insulated from its surroundings, and the material properties are constant), we have shown that the Rosenthal solution can be used to give a reasonable approximation of the temperature profile in the HAZ [6]. For laser welding, this type of approach cannot be used due to the nature of the power beam process. However, recently a thermal model has been developed which has been validated for the laser welding of thin sheet Al alloys [5]. In this model the heat input is described in terms of a point and line source.

In Fig. 4, typical outputs of both models are displayed in the form of peak temperatures as a function of distance from the weld centreline, for representative TIG and laser welds at one welding speed. For the alloy 2024, the liquidus and solidus temperatures have been reported to be 640°C and 504°C respectively and are marked on Fig. 4. In laser welding, the power source is very focused producing very high peak

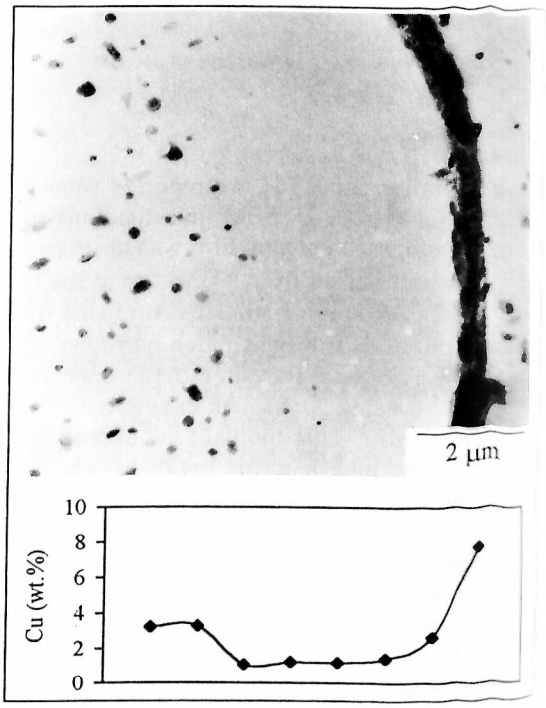

Figure 3: *(a) TEM micrograph showing a region of grain boundary melting, and (b) plot of Cu concentration.*

temperatures in the fusion zone, compared to TIG welding where there is considerable spread of the arc. However, in the HAZ, the narrow focused laser beam has the advantage of producing higher cooling rates which results in the peak temperature decreasing at a faster rate compared to the TIG welds. As can be seen from Fig. 4, the distance over which the peak temperature is in the melting range for the alloy AA2024 is predicted to be ~ 400 μm for the laser weld and ~ 1 mm for the TIG weld. Although the models correctly predict that the width of the region of grain boundary melting is narrower for the laser welds compared to the TIG welds, they both overestimate the width of the region by almost double that determined experimentally.

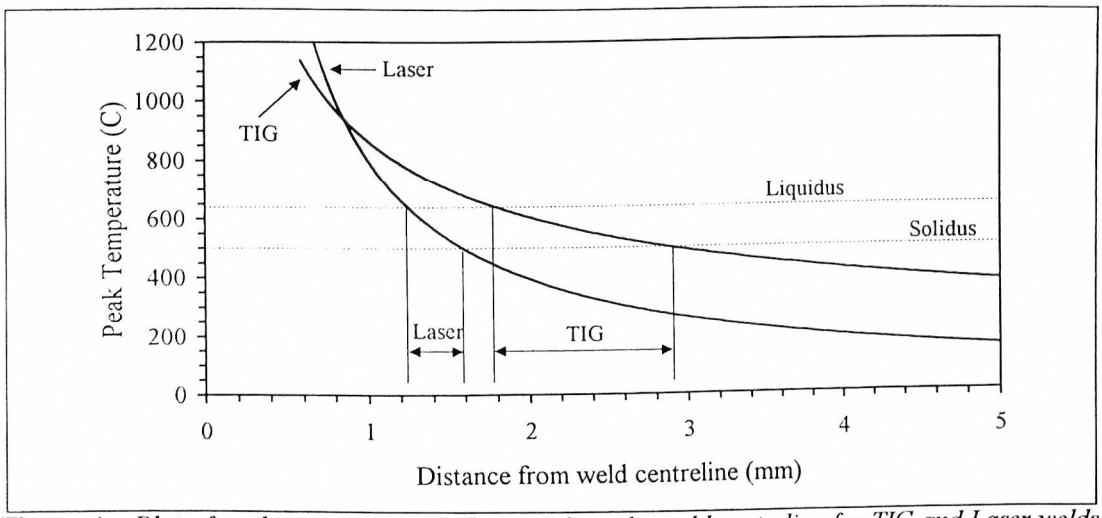

Figure 4: *Plot of peak temperature vs. distance from the weld centreline for TIG and Laser welds (welding speed = 33 mm s^{-1}). Also indicated on the plot is the width for the potential to form grain boundary melting.*

This difference could be due to two possible reasons. Firstly, in both the thermal models, assumptions are made which do not take into account the effect of any loss in heat to the surroundings. In practice, it is necessary to use large clamping plates to prevent the sheet metal from moving during the welding operation. Clearly, the presence of the clamps will act as heat sinks and effectively increase the cooling rate in the solid state, i.e. the curves shown in Fig. 4 are likely to be steeper thus reducing the width of the region of grain boundary melting. Secondly, the reported solidus of 2024 (504°C) is for cast material where the θ, S and α ternary eutectic phases are all present in intimate contact in the microstructure prior to melting. This is not the case for the rolled product which has been homogenised and recrystallised during thermomechanical processing, as the majority of the eutectic is dissolved and redistributed throughout the microstructure. Unless the S and θ phases precipitate at the grain boundaries in intimate contact during the heating cycle, it is reasonable to expect that in welding, partial melting will not initiate at 504°C but at a somewhat higher temperature. This will narrow the effective freezing range of the alloy and reduce the width of the region of grain boundary melting.

Preliminary studies using sheet material of 2024 heated to different temperatures above 500°C in an air furnace and DSC found that grain boundary melting of the homogenised sheet occurs at ~ 520°C. However this may be sensitive to heating rate, due to the requirement for both θ and S phases to be present and in intimate contact at the grain boundaries for the melting point to be depressed to that of the ternary eutectic temperature.

4. Conclusions

1. The heat affected zones were investigated for two fusion welding processes, namely TIG and laser beam. A region of grain boundary melting was observed in all the weld samples and was associated with the formation of a precipitate free zone and coarse spherical particles of the equilibrium S phase.
2. The focused power source, and associated high cooling rates of laser welding produced a narrow region of grain boundary melting (100-200 μm) whereas for the TIG welds, in which an arc is utilised, the cooling rates in the solid state are much lower producing a wide region of grain boundary melting (~ 500 μm).
3. Thermal models were used to successfully predict the trend of grain boundary melting with welding technique. However some difficulties were encountered in accurately predicting the width of the region of grain boundary melting. In particular the effects of jigging need to be taken into account.
4. Furthermore the local grain boundary melting temperature of the homogenised rolled sheet material needs to be accurately determined at high heating rates as it appears to be significantly higher than the quoted values for cast structures.

5. Acknowledgements

This work was supported by the EPSRC under the IMI Programme, Grant: GR/K66901, and is released with the kind permission of the following partners: British Aerospace, Short Brothers, DERA, Rolls Royce, British Aluminium, TWI, University of Liverpool, Cranfield University and the University of Essex.

6. References

[1] S. Kou: Welding Research Council Bulletin, 320 (1986), 1.
[2] A.F. Norman and P.B. Prangnell: submitted to Mat Sci. Eng. A.
[3] S. Kou and Y. Le: Welding Journal, 65 (1986), 305s.
[4] T. Ganaha, B.P. Pearce and H.W. Kerr: Metallurgical Transactions A, 11 (1980), 1351.
[5] A.F. Norman, R. Ducharme, A. mackwood, P. Kapadia and P.B. Prangnell: Science and Technology of Welding and Joining, in press.
[6] A.F. Norman, V. Drazhner, N. Woodward and P.B. Prangnell: Proc. 7th Int. Conf. on Joints in Aluminium (INALCO '98), Cambridge, April 1998, in press.
[7] ASM Speciality Handbook: Aluminium and Aluminium Alloys, (edited by J.R. Davis), ASM International, p. 376 (1993).
[8] S.L. Chen, Y. Zuo, H. Liang and Y.A. Chang: Metallurgical Transactions A, 28 (1997), 435.
[9] D. Rosenthal: welding Journal, 20 (1941), 220s.